Synthesis and Biological Evaluation of New Geiparvarin Derivatives

Stefano Chimichi,[b] Marco Boccalini,[b] Alessia Salvador,[c] Francesco Dall'Acqua,[c] Giuseppe Basso,[a] and Giampietro Viola*[a]

New geiparvarin derivatives modified at the unsaturated alkenyloxy bridge, where a hydrogen atom replaces the 3′-methyl group, were synthesized and evaluated against a panel of human tumor cell lines in vitro. These compounds demonstrated an increase in growth inhibitory activity relative to the parent compound, geiparvarin. The activity increased even further in the series of demethylated compounds, with the introduction of a methyl group at the 1′-position of the alkenyloxy chain. In contrast, a remarkable decrease in activity was observed with the introduction of a methyl group at the 2′-position. Interestingly, the new derivatives fully inhibited the growth of drug-resistant cell lines, suggesting that they are not subject to pump-mediated drug efflux. On the basis of their cytotoxic profiles, the most active compounds (R)-4 and (R)-5 were selected for further biological evaluation in comparison with the lead compound. The new derivatives strongly induce apoptosis in a promyelocytic leukemia cell line (HL-60) mediated by depolarization of mitochondrial transmembrane potential and mitochondrial production of reactive oxygen species (ROS).

Introduction

Geiparvarin (1, Figure 1) is a natural coumarin isolated from the leaves of *Geijera parviflora* that has been found to exhibit antiproliferative activity against several tumor cell lines.[1–3] With the goal of increasing this activity, various modifications of the basic geiparvarin structure have been made over the past few years. Unfortunately, most attempts resulted in a loss of activity, or at best, only a slight improvement.[4–6] The relative importance of aspects of the geiparvarin structure, such as the 3(2H)-furanone ring, the coumarin group, and the alkenyloxy bridge, has been studied extensively without conclusive results. In particular, the alkenyloxy bridge has been modified to 1,3-butadiene[5] or spaced from the furanone ring by a terpenoid unit,[6] but neither of these modifications has given rise to compounds as active as geiparvarin.

We demonstrated that demethylation of geiparvarin in its alkenyloxy bridge led to a series of compounds endowed with increased cytotoxic activity.[7,8] In pursuing our interest in the synthesis and biological evaluation of geiparvarin derivatives and on the basis of our previous results, we report herein the synthesis of some new geiparvarin analogues. Moreover, we describe their evaluation against a panel of human tumor cell lines in vitro together with detailed experiments designed to elucidate the mechanism(s) of their antiproliferative effect.

Results and Discussion

Chemistry

Few years ago we described the facile and convenient synthesis of 7-(2-oxoethoxy)coumarins and of racemic 2-[(coumarin-7-yl)oxy]propanal (10) in excellent overall yields (97 %).[9] On this basis and following our preliminary results,[10] we now report the synthesis of enantiomerically pure aldehydes (R)- and (S)-
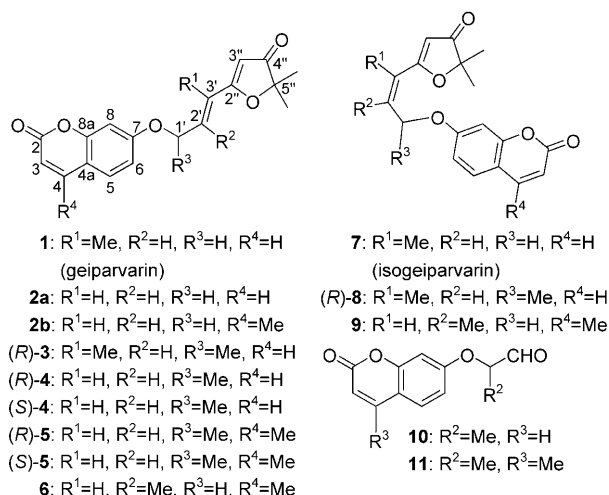

Figure 1. Geiparvarin analogues and their intermediates.

1: R^1=Me, R^2=H, R^3=H, R^4=H (geiparvarin)
2a: R^1=H, R^2=H, R^3=H, R^4=H
2b: R^1=H, R^2=H, R^3=H, R^4=Me
(R)-3: R^1=Me, R^2=H, R^3=Me, R^4=H
(R)-4: R^1=H, R^2=H, R^3=Me, R^4=H
(S)-4: R^1=H, R^2=H, R^3=Me, R^4=H
(R)-5: R^1=H, R^2=H, R^3=Me, R^4=Me
(S)-5: R^1=H, R^2=H, R^3=Me, R^4=Me
6: R^1=H, R^2=Me, R^3=H, R^4=Me

7: R^1=Me, R^2=H, R^3=H, R^4=H (isogeiparvarin)
(R)-8: R^1=Me, R^2=H, R^3=Me, R^4=H
9: R^1=H, R^2=Me, R^3=H, R^4=Me

10: R^2=Me, R^3=H
11: R^2=Me, R^3=Me

[a] Prof. G. Basso, Dr. G. Viola
University of Padova, Department of Pediatrics
Laboratory of Oncohematology, Via Giustiniani 3, 35131 Padova (Italy)
Fax: (+ 39) 49-821-1452
E-mail: giampietro.viola.1@unipd.it

[b] Prof. S. Chimichi, Dr. M. Boccalini
University of Firenze, Department of Organic Chemistry
Via della Lastruccia 13, 50019 Sesto Fiorentino (Italy)

[c] Dr. A. Salvador, Prof. F. Dall'Acqua
University of Padova, Department of Pharmaceutical Sciences
Via Marzolo 5, 35131 Padova (Italy)

10 and (*R*)- and (*S*)-**11** by starting from the readily available 7-hydroxycoumarins, with the aim to synthesize the optically active geiparvarin analogues **3–5** and **8** as well as compounds **6** and **9** (Figure 1).

As various attempts to resolve the mixture of Schiff bases obtained from (*R,S*)-**10** by reaction with an enantiomerically pure amine failed, a different resolution method is required to obtain enantiomerically pure aldehyde **10** on a large scale. Enantiomerically pure (*R*)- and (*S*)-**10** were obtained by the sequence outlined in Scheme 1: resolution of the racemic coumarinyloxypropionic acid **12**[9] was achieved by its condensation with an enantiomerically pure alcohol or amine with subsequent separation and hydrolysis of the resulting diastereomers to give, after Rosenmund reduction, the required aldehydes. In particular, a mixture of diastereomeric esters **13a** and **13b** (*de* ~ 20%) was obtained by reaction of the acid chloride of **12** with (1*R*,2*S*,5*R*)-(−)-menthol. Although this mixture afforded a single spot in thin-layer chromatography with differ-
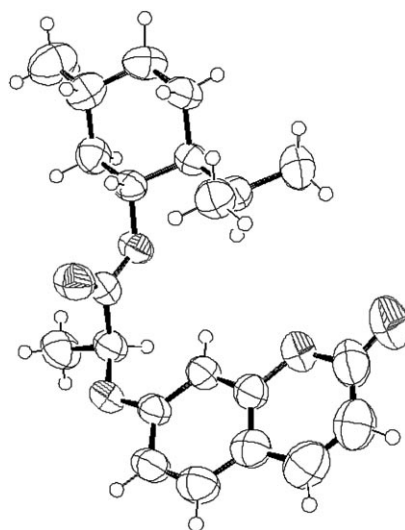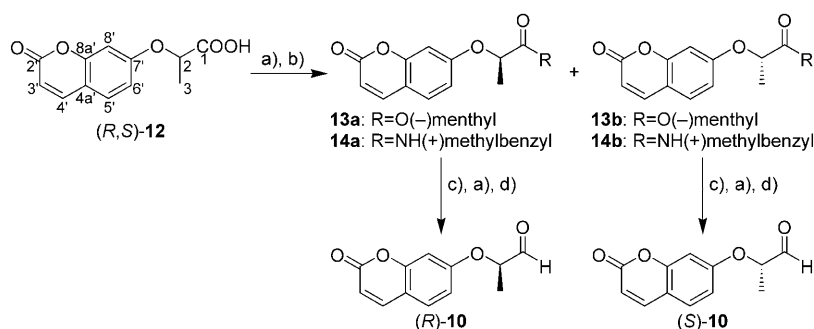

Figure 2. ORTEP drawing for compound **13b**.

Scheme 1. Synthesis of intermediates for the preparation of geiparvarin analogues: a) SOCl$_2$, CHCl$_3$, reflux; b) (1*R*,2*S*,5*R*)-(−)-menthol or (1*R*)-(+)-1-phenylethanamine (α-methylbenzylamine), CHCl$_3$, reflux; c) NaOH, CH$_3$CN, room temperature or 6 m HCl, reflux; d) H$_2$, Pd/BaSO$_4$, toluene.

ent eluents, one diastereomer easily crystallized quantitatively from ethanol. The absolute configuration at C2 was ascertained to be *S* (compound **13b**), with respect to the chiral carbon atoms of menthol on the basis of X-ray crystallographic analysis (Figure 2). The remaining mother liquors containing almost exclusively **13a** were subjected again to crystallization to give the required compound (see Experimental Section).

Treatment of the ester **13a** or **13b** with an alcoholic solution of sodium hydroxide at room temperature only afforded the racemic acid **12**. A convenient enantiomeric excess of the acid (> 98% *ee*) was achieved when the hydrolysis was performed in acetonitrile with a 10% aqueous solution of sodium hydroxide or potassium hydroxide at room temperature for five days.

Optical resolution of the racemic **12** could also be attained by reaction of the corresponding acyl chloride with (1*R*)-(+)-1-phenylethanamine to give the amides **14a,b** (*de* ~ 10%) (Scheme 1). Once again, separation of the diastereomeric amides **14a,b** was achieved by fractional crystallization from methanol/water. Subsequent hydrolysis with 6 m hydrochloric acid gave the enantiomerically pure acids; the structure of (*R*)-

**12** was determined by comparison of its specific rotation [α] with that of the previously obtained sample.

The optical isomers (*R*)- and (*S*)-**16** were also obtained by an enantioselective synthesis (Mitsunobu reaction),[11] which allows a ready assignment of the absolute configuration. Thus, we started by condensing (*S*)-ethyl- or (*R*)-isobutyl lactate with 7-hydroxy-4-methylcoumarin (**15**). It is well known that this reaction affords the corresponding esters with inversion of configuration; the esters dissolved in methanol were then hydrolyzed with 10% sodium hydroxide followed by acidification with 2.4 m hydrochloric acid to pH 2 to give the acids (*R*)- or (*S*)-**16**, respectively (no racemization was observed; Scheme 2).

Finally, application of our methodology[9] to the preparation of the enantiomerically pure acids **12** and **16** indicated that the temperature was the most important factor in the reduction of the corresponding acyl chlorides; good yields of aldehydes **10** and **11** (80–90%) were obtained only if the reaction temperature was kept < 130 °C, the temperature at which hydrogen chloride begins to evolve.

Notably, this approach to enantiomerically pure aryloxy aldehydes avoids the drawback of enantioselective hydroformylation of aryl vinyl ethers employing a chiral rhodium complex, in which the obtained chiral non-racemic aldehyde racemizes during the reaction.[12] Therefore, the reduction of the acyl chlorides of enantiomerically pure acids **12** and **16** represents a novel strategy to enantiomerically pure aryloxy aldehydes.
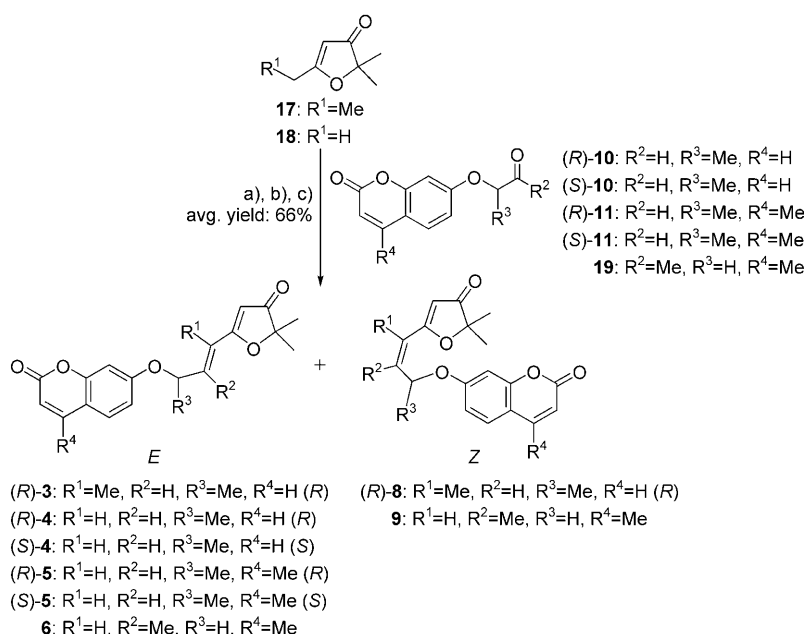
The easy access to enantiomerically pure aldehydes **10** and **11** allowed us to synthesize chiral geiparvarin analogues by condensation with 5-substituted 2,2-dimethyl-3(2*H*)-furanones
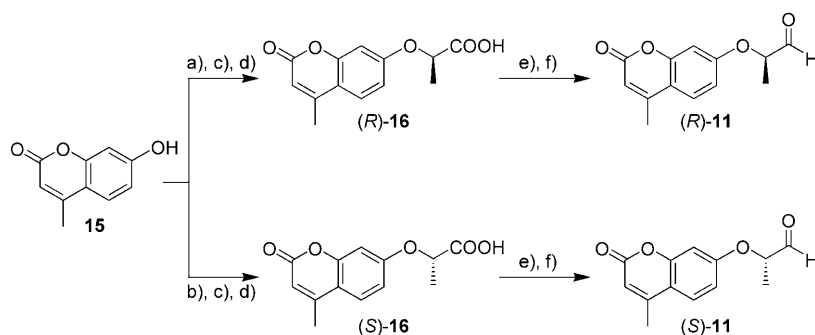
Scheme 2. Synthesis of intermediates for the preparation of geiparvarin analogues: a) ethyl-(2S)-hydroxypropanoate, PPh₃, DIAD, THF, room temperature; b) isobutyl-(2R)-hydroxypropanoate, PPh₃, DIAD, THF, room temperature; c) NaOH (1.25 M), CH₃OH, room temperature; d) HCl (2.4 M); e) SOCl₂, CHCl₃, reflux; f) H₂, Pd/BaSO₄, toluene.

(17 and 18) followed by dehydration of the intermediate aldols (Scheme 3). The same procedure carried out on ketone 19 afforded the new derivatives 6 and 9.

Scheme 3. Synthesis of geiparvarin analogues: a) LDA, THF, −78 °C; b) 10 or 11 or 19, THF; c) MeSO₂Cl, Et₃N, THF, 0 °C.

Assignment of the configuration of the 2′–3′ double bond in compounds 4 and 5 was achieved on the basis of H-2′–H-3′ vicinal coupling constant values (~16 Hz) determined by ^{1}H NMR spectra. For compounds 6 and 9, and 3 and 8, the long-range coupling constant between H-3′ and the 2′ methyl group in 6 and 9 (or H-2′ and 3′-Me in 3 and 8) is not diagnostic for structural determination (^4J cisoid≅^4J transoid). Stereochemistry of the products was therefore determined by NOE experiments. To this end, we assigned the alkenyloxy signals of H-3′ and 2′-Me in compounds 6 and 9 (or H-2′ and 3′-Me in compounds 3 and 8) on the basis of 2D NMR experiments (gHSQC and gHMBC). Irradiation, for example, of the signal at $\delta = 6.33$ ppm

(attributed to H-3′ in the compound at lowest R_f) gives rise to a significant enhancement on the 1′-CH₂ protons, thus confirming the E configuration of compound 6 (Figure 3a). Analogously, irradiation of the signal at $\delta = 6.22$ ppm (H-3′) of the compound at the highest R_f leads to a significant enhancement on the 2′-Me protons, thus allowing us to assign the Z configuration to compound 9 (Figure 3b). This result was also confirmed by the expected and significant difference ($\Delta\delta = 5.62$ ppm) in the ^{13}C NMR chemical shifts between the resonances of the methyl group at the 2′-position ($\delta = 22.32$ ppm in the Z stereoisomer versus $\delta = 16.70$ ppm in the E isomer).

Biology

Antiproliferative activity

The new geiparvarin derivatives were evaluated for their inhibitory effects on the proliferation of a panel of human tumor cell lines after incubation for 72 h. The results are reported in Table 1 (compounds 1 and 2a are included as reference).

The introduction of a methyl group at position 1′ of geiparvarin (1) led to compounds (R)-3 and (R)-8, which lost activity regardless of respective E or Z configuration. As previously demonstrated, demethylation of the lead compound 1 led to compound 2a, which exhibits a significant increase in antiproliferative activity.[7,8] The introduction of a methyl group at position 1′ of 2a gives two enantiomers, (R)-4 and (S)-4, which exhibited a slight increase in activity. Interestingly, antiproliferative activity does not depend on the configuration at the 1′ carbon atom.

Introduction of a methyl group at position 4 of the coumarin ring of compounds (R)-4 and (S)-4 gives (R)-5 and (S)-5, respectively; all these compounds show the same cytotoxicity, suggesting that the coumarin moiety is not essential to this end, as previously postulated.[4–6]
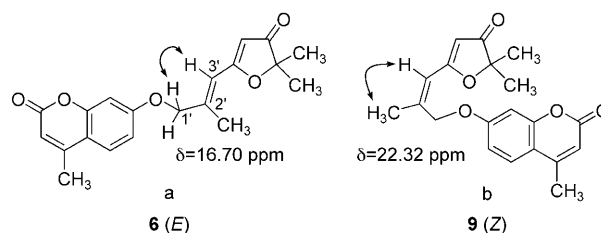

Figure 3. Significant NOE effects in compounds 6 and 9.

These are not the final page numbers! ⇗⇗

Table 1. Growth inhibitory activity of geiparvarin derivatives against a panel of human tumor cell lines.

Compd	Cell lines; GI_{50} [μM][a]						
	HL-60	Jurkat	CEM	K562	LoVo	HT-1080	MCF7
1	6.3 ± 0.6	1.8 ± 0.2	1.8 ± 0.6	9.2 ± 0.5	9.2 ± 1.3	9.8 ± 0.9	6.0 ± 0.7
2a	2.5 ± 0.2	0.6 ± 0.05	0.7 ± 0.9	4.8 ± 0.2	4.1 ± 0.1	6.9 ± 0.6	3.4 ± 0.3
(R)-**3**	>10	>10	>10	>10	>20	>20	11.5 ± 0.5
(R)-**4**	0.7 ± 0.01	0.8 ± 0.02	0.7 ± 0.3	1.3 ± 0.1	3.2 ± 0.4	2.9 ± 0.1	2.4 ± 0.8
(S)-**4**	0.9 ± 0.01	0.5 ± 0.01	1.0 ± 0.1	1.6 ± 0.3	2.7 ± 0.3	2.1 ± 0.1	2.5 ± 0.6
(R)-**5**	0.5 ± 0.02	0.3 ± 0.02	0.4 ± 0.1	0.5 ± 0.01	2.5 ± 0.2	4.4 ± 0.2	4.5 ± 0.4
(S)-**5**	0.8 ± 0.01	0.4 ± 0.01	0.7 ± 0.2	0.6 ± 0.02	2.7 ± 0.3	4.4 ± 0.5	2.5 ± 0.3
6	>10	>10	4.3 ± 0.9	>10	>20	>20	6.8 ± 0.9
(R)-**8**	>10	>10	>10	>10	>20	>20	13.4 ± 0.9
9	>10	>10	6.1 ± 0.5	>10	>20	>20	16.0 ± 1.9

[a] GI_{50}: concentration at which 50% growth inhibition of tumor cells is observed after 72 h incubation; values represent the mean $\pm$ SEM of three independent experiments.

P-gp, are endowed with a second type of multidrug resistance associated with the upregulation of glutathione transferase and glutathione peroxidase. Thus MCF7-MDR cells are known to possess both efflux pumps as well as increased levels of glutathione peroxidase activity.[17] In agreement with our previous results[8] in which we showed that **1** and **2a** retain activity in multidrug-resistant cells, the new compounds also proved to be fully inhibitory to these resistant cell lines, as shown in Table 2, suggesting that they are not subject to the pump-mediated efflux of antitumor drugs.

Introduction of the methyl group at position 2′ of compound **2b** gives the two diastereomers **6** and **9**. A remarkable decrease in activity was observed with these compounds, irrespective of the *E* or *Z* configuration. Altogether, these data indicate that the presence of a methyl group at the double bond strongly decreases the antiproliferative activity and simultaneously suggests that this part of the molecule plays a major role with respect to the coumarin moiety or to the furanone ring.

Table 2. Effect of geiparvarin derivatives against various drug-resistant cell lines.

Compd	Cell lines; GI_{50} [μM][a]					
	CEM	CEM-VBL10	MCF7	MCF7-MDR	LoVo	LoVo/Doxo
(R)-**4**	0.7 ± 0.1	0.8 ± 0.1 (1.1)	2.4 ± 0.2	3.0 ± 0.5 (1.2)	3.2 ± 0.5	1.9 ± 0.1 (0.6)
(S)-**4**	1.0 ± 0.01	0.3 ± 0.03 (0.3)	2.5 ± 0.3	2.9 ± 0.3 (1.2)	2.7 ± 0.2	1.6 ± 0.1 (0.6)
(R)-**5**	1.3 ± 0.2	1.7 ± 0.2 (1.3)	4.5 ± 0.4	4.0 ± 0.6 (0.9)	2.5 ± 0.4	2.5 ± 0.2 (1.0)
(S)-**5**	0.6 ± 0.1	0.3 ± 0.05 (0.5)	2.8 ± 0.3	3.1 ± 0.3 (1.1)	2.7 ± 0.2	1.9 ± 0.2 (0.7)
vinblastine	0.004 ± 0.0002	0.21 ± 0.03 (525)	0.006 ± 0.001	0.5 ± 0.09 (83)	ND	ND
doxorubicin	ND	ND	0.2 ± 0.08	20.2 ± 1.5 (101)	0.12 ± 0.03	13.5 ± 0.2 (112.5)

[a] GI_{50}: concentration at which 50% growth inhibition of tumor cells is observed after 72 h incubation; values represent the mean $\pm$ SEM of three independent experiments. Values in brackets are the fold resistance, which indicates the decreased potency of the compound in the resistant cell line. ND: not determined.

Effect of geiparvarin derivatives on multidrug-resistant cell lines

Although many anticancer drugs in clinical use are effective for the treatment of various tumor types, their potential is limited by the emergence of drug resistance. Resistance can be intrinsic or acquired, but in either case, tumors become refractory to a variety of structurally diverse drugs. Therefore, we investigated the inhibitory activity of the most potent compounds **1**, **2a**, (R)-**3**, and (R)-**5** against drug-resistant cell lines. We used the human colon adenocarcinoma cell line (LoVo) and its doxorubicin-resistant subline (LoVo/Doxo); this cell line is resistant to a number of intercalating agents such as various anthracyclines, mitoxantrone, and ametantrone.[13, 14] CEM, a leukemic T-lymphocyte line, and its subline, CEM-VBL10, were selected for by continuous treatment with vinblastine; they show a classical multidrug-resistance phenotype and overexpress the *mdr1* gene.[15] MCF7-MDR is a human mammary carcinoma cell line that exhibits multidrug resistance and a high-level expression of P-glycoprotein (P-gp). MCF7-MDR cells show cross-resistance to multiple structurally unrelated drugs including anthracyclines, vinca alkaloids, epipodophyllotoxins, actinomycin D, and colchicines.[16] These cells, in addition to the overexpression of

Treatment with geiparvarin derivatives induces externalization of phosphatidylserine in HL-60 cells

Apoptosis is characterized by a variety of morphological transformations. Changes to the plasma membrane are among the earliest of these events.[18] In apoptotic cells, the membrane phospholipid phosphatidylserine (PS) is translocated from the inner to the outer leaflet of the plasma membrane, thereby exposing PS to the external cellular environment. Annexin V is a 35–36 kDa Ca^{2+}-dependent phospholipid binding protein that has high affinity for PS and binds to cells with exposed PS. We performed bi-parametric cytofluorimetric analysis using propidium iodide (PI) and annexin V–FITC conjugates, which stain DNA and PS residues respectively.[19] Figure 4 shows the percentage of annexin V-positive cells after incubation of HL-60 cells in the presence of **1**, **2a**, (R)-**4**, and (R)-**5** at various concentrations for 24 h. A concentration-dependent induction of apoptotic cells is observed in particular for compounds (R)-**4** and (R)-**5**, in good agreement with cytotoxic potency.

Cell-cycle analysis

Treatment of HL-60 cells with increasing drug concentrations led to profound changes in the cell-cycle profile (Figure 5A
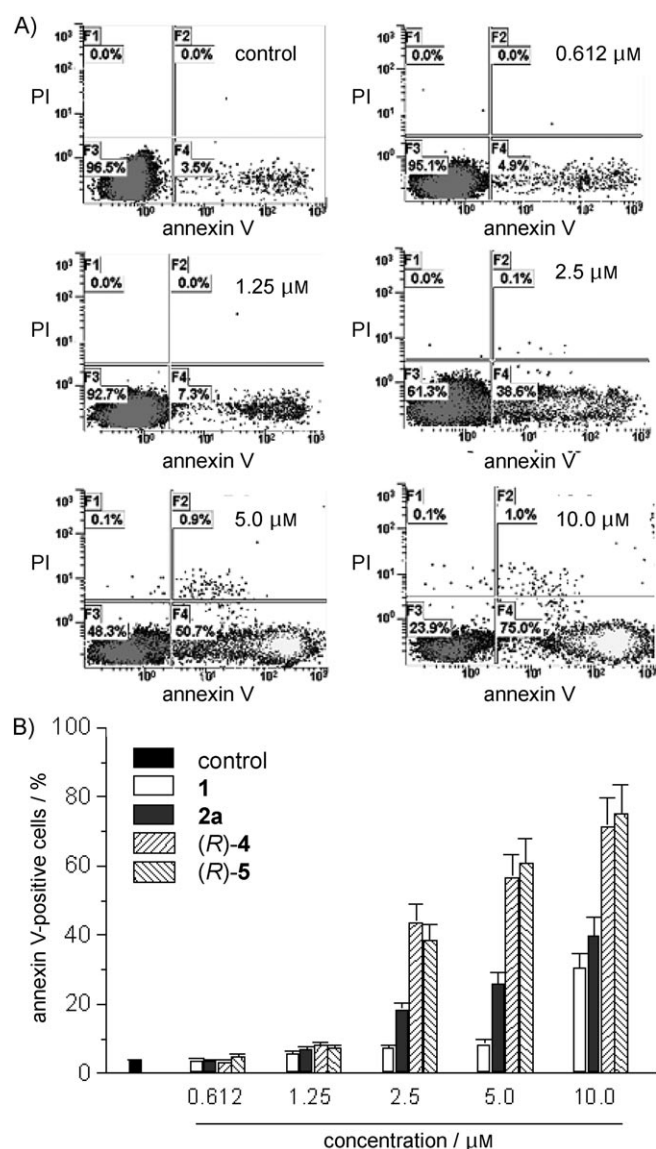
Figure 4. A) Representative bi-parametric histograms of HL-60 cells treated with increasing concentrations (indicated) of compound (*R*)-**5**, and then stained with PI and annexin V–FITC after 24 h incubation. B) Percentage of annexin V-positive cells for compounds **1**, **2a**, (*R*)-**4**, and (*R*)-**5** at various concentrations after 24 h incubation. Data are expressed as the mean ± SEM of three independent experiments.

Figure 5. Cell-cycle analysis of HL-60 cells incubated for 24 h with increasing concentrations of A) **1** and B) (*R*)-**5**, as indicated. Cells were fixed and labeled with PI and analyzed by flow cytometry as described in the Experimental Section.

and B). Flow cytometric analysis of PI-labeled cells after incubation with the test compounds for 24 h indicated that untreated cells show a classic pattern of proliferation, with proportional distribution across G_1 (40%), S (47%), and G_2M (13%) phases (Figure 6 A). Treatment with low concentrations of **1** and **2a** (1.0–5.0 μM) induced a remarkable concentration-dependent accumulation of cells in the G_1 phase 24 h followed by accumulation in the G_2M phase at higher concentrations (10–15 μM). A concomitant decrease in S-phase cells was also observed. Compound (*R*)-**4** induces, at lower concentrations (1–2 μM), a slight increase in the G_1 phase from 40 to 50%, followed at higher concentrations by accumulation in the S phase. In contrast, no G_1 arrest pattern was observed with (*R*)-
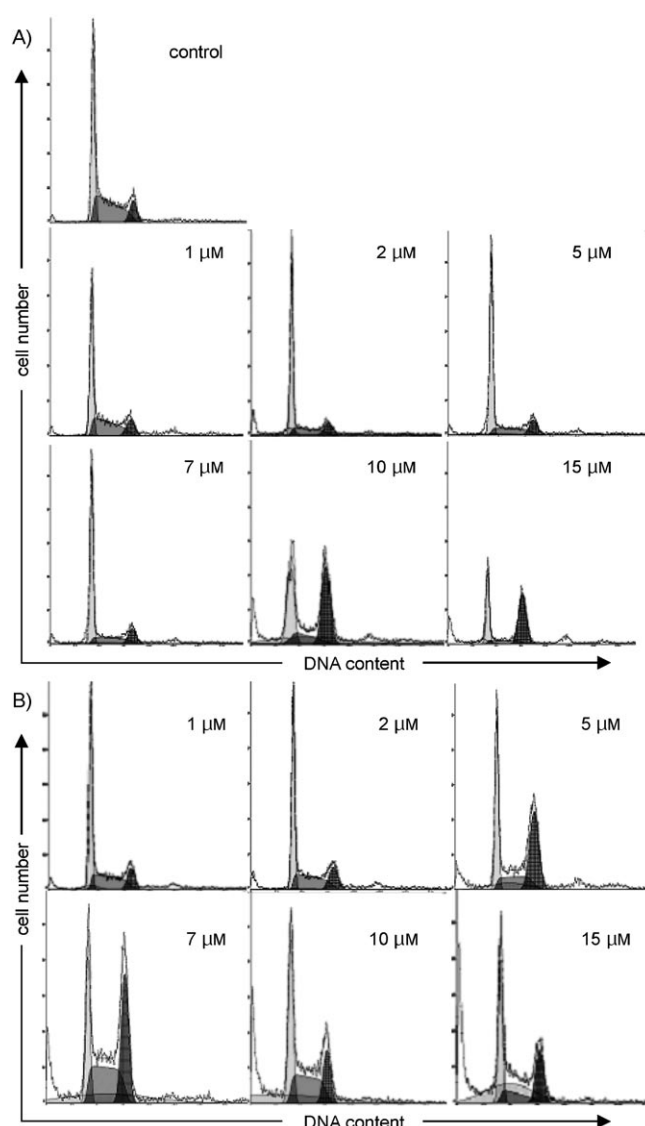
5, but only a G_2M block that occurs at 5 μM. Interestingly, the percentage of the cell population with a hypodiploid DNA content peak (sub-G_1), usually considered as apoptotic cells, is concentration dependent for (*R*)-**4** and (*R*)-**5**, reaching 40–60% at the highest concentrations tested (Figure 6 B). The other compounds **1** and **2a** induced a significant percentage of apoptotic cells at the highest concentrations used (10–15 μM). This effect of geiparvarin derivatives on the cell cycle has not been described before. A previous publication[20] reports that geiparvarin (**1**) had no effect on the cell cycle of murine 3T3 fibroblasts, even at concentrations higher (100 μM) than those used in the present study. This discrepancy could be explained by geiparvarin eliciting a different response in tumor cells used in this study as opposed to a non-tumor cell line such as murine fibroblasts.
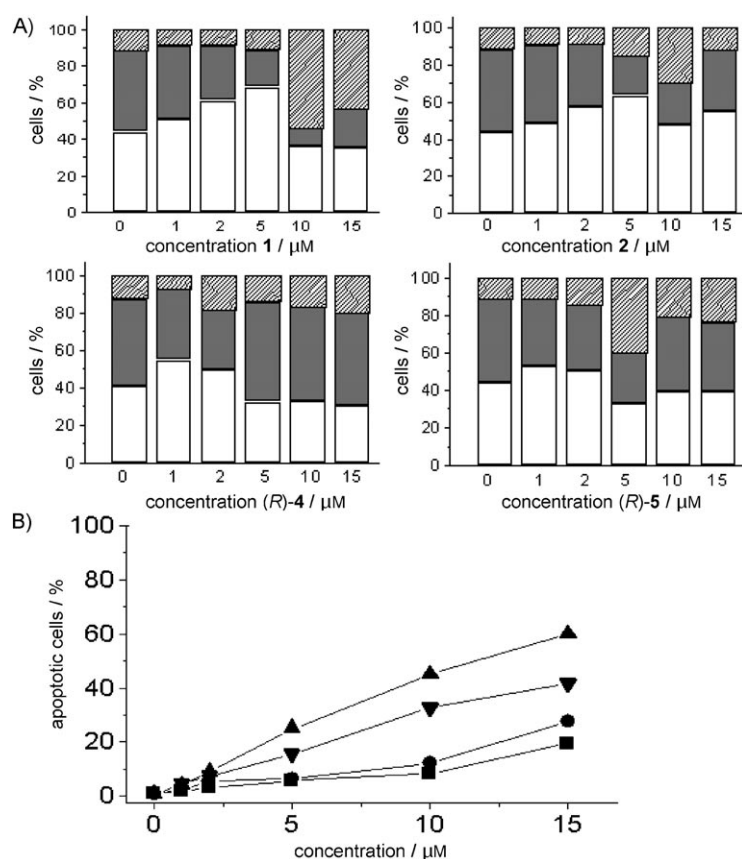
These are not the final page numbers! ↗↗

Figure 6. A) Percentage of HL-60 cells at various cell-cycle phases after 24 h incubation in the presence of **1**, **2a**, (R)-**4**, and (R)-**5** at the concentrations indicated. The percentage of each phase of the cell cycle (G$_1$, white bars; S, gray bars; G$_2$M, shaded bars) were calculated on living cells. B) Percentage of the cell population with hypodiploid DNA content peak (apoptotic cells) after 24 h incubation in the presence of **1** (■), **2a** (●), (R)-**4** (▲), and (R)-**5** (▼) at the indicated concentrations.

Geiparvarin derivatives induce depolarization of mitochondrial transmembrane potential

As demonstrated above, geiparvarin treatment induces apoptosis. This observation prompted us to investigate the activation of the apoptotic pathway after treatment. Impairment in mitochondrial function is an early event in the executive phase of programmed cell death in various cell types, and appears as the result of a preliminary decrease in the mitochondrial transmembrane potential ($\Delta\psi_{mt}$).[21,22] Early ψ_{mt} disruption would result from the opening of mitochondrial permeability transition pores (PTP), and this permeability transition would trigger the release of apoptogenic factors such as apoptosis-inducing factor (AIF) or cytochrome *c*, capable of inducing downstream apoptotic events.[21,22]

We used the lipophilic cation 5,5′,6,6′-tetrachloro-1,1′,3,3′-tetraethylbenzimidazolcarbocyanine (JC-1) to monitor $\Delta\psi_{mt}$ induced by the test compounds. The method is based on the ability of this fluorescent probe to selectively enter mitochondria, as it reversibly changes from green to orange with increasing transmembrane potential.[23] This property is due to the reversible formation of JC-1 aggregates upon membrane polarization that causes a shift in the emitted wavelength from

530 nm (i.e. λ_{em} of JC-1 in monomeric form) to 590 nm (λ_{em} of JC-1 aggregate) when excited at 490 nm. HL-60 cells were treated with **1**, **2a**, (R)-**4**, and (R)-**5** at various concentrations for 24 h. Treated cells exhibited a dramatic and concentration-dependent shift in fluorescence relative to control cells, indicating depolarization of ψ_{mt} (Figure 7A).

Depolarization of ψ_{mt} is particularly evident for compounds (R)-**4** and (R)-**5** (Figure 7B). Notably, the disruption of ψ_{mt} is associated with the appearance of annexin V in treated cells, where they are in the early stages of apoptosis. In fact, dissipation of ψ_{mt} is characteristic of apoptosis, and has commonly been observed with a variety of anticancer drugs irrespective of cell type.

Geiparvarin derivatives induce mitochondrial production of ROS

Mitochondrial transmembrane potential depolarization has been associated with mitochondrial production of reactive oxygen species (ROS).[24–26] To investigate the effects of geiparvarin derivatives on the production of ROS during apoptosis, we used the ROS-specific fluorescence indicator hydroethidine (HE), which fluoresces in the presence of ROS.[27,28] The results are depicted in Figure 8A and B. In agreement with the depolarization of ψ_{mt}, significant ROS effects were observed particularly for compounds (R)-**4** and (R)-**5** in a concentration-dependent manner.

In parallel, we evaluated the damage produced by ROS in mitochondria by assessing the oxidation state of cardiolipin, a phospholipid restricted to the inner mitochondrial membrane. We used 10-*N*-nonyl-acridine orange (NAO), a fluorescent probe that is independent of transitions in mitochondrial membrane permeability.[29,30] The dye interacts stoichiometrically with intact non-oxidized cardiolipin. Therefore, oxidative stress localized to mitochondria can be assessed by measuring NAO fluorescence. Treated HL-60 cells showed a progressive and remarkable decrease in mean NAO fluorescence with increasing concentrations of the four compounds, consistent with a loss of cardiolipin content (Figure 9A and B).

Conclusions

In pursuing our line of research into the medicinal chemistry of geiparvarin, we have attempted to further improve the basic properties of the parent compound through selected structural modifications at the alkenyloxy bridge. The introduction of a methyl group at position 1′ of compound **2a** increases the antiproliferative activity. Interestingly, this effect is not stereospecific. Further flow cytometric experiments identified the new derivatives (R)-**4** and (R)-**5** as potent inducers of apoptosis in human leukemic HL-60 cells. Compounds (R)-**4** and (R)-**5** induced annexin V-positive cells in a dose-dependent manner. Importantly, the induction of apoptosis was also con-
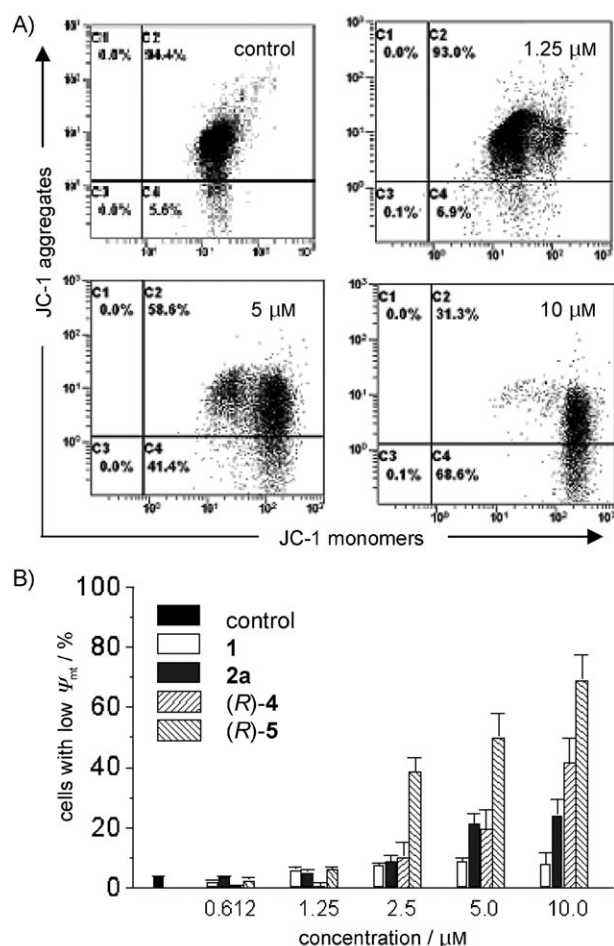
Figure 7. Induction of the loss of mitochondrial transmembrane potential in HL-60 cells by test compounds after 24 h incubation. A) Representative histograms of cells incubated in the presence of (*R*)-**5** at the indicated concentrations and then stained with the fluorescent probe JC-1; horizontal axes show the fluorescence intensity of the JC-1 monomer, and vertical axes show the fluorescence of JC-1 aggregates. B) Percentage of cells with low ψ_{mt} for compounds **1**, **2a**, (*R*)-**4**, and (*R*)-**5** after 24 h incubation; data are expressed as the mean ± SEM for three independent experiments.

firmed by the analysis of the cell cycle. In fact, concentrations lower than 2.5 μM are sufficient to induce generation of hypodiploid (apoptotic) cells. For comparison, elevated levels of cells in sub-G_1 were observed only for concentrations greater than 10 μM for the lead compound **1**.

Malignant tumors can be resistant to treatment with chemotherapeutic drugs, and the mechanism of this resistance is often mediated by overexpression of the 170 kDa P-glycoprotein drug efflux pump. The most active compounds (*R*)-**4** and (*R*)-**5** also exhibited cytotoxic activity against the drug-resistant cell lines CEM-VBL10 and LoVo/Doxo, which overexpress P-gp. These results suggest that these compounds may be useful in the treatment of drug-refractory tumors.

The apoptotic death induced by geiparvarin derivatives is associated with important changes in mitochondrial function such as dissipation of the transmembrane potential and generation of ROS. The dissipation of ψ_{mt} is associated with the appearance of apoptotic cells; it is well established that commit-

ment to apoptosis can involve important changes in mitochondrial activity.

The precise targets involved in the apoptotic mechanism remain unclear at present. Further investigations are needed to identify the initial signal(s) as well as the molecular targets. Identification of these specific targets may improve the biological activity of geiparvarin, and in this context, investigations are currently underway.

Experimental Section

General methods: Melting points were taken on a Büchi 510 apparatus and are uncorrected. Elemental analyses were obtained with a PerkinElmer 240C elemental analyzer. MS data were collected with a Carlo Erba QMD 1000 instrument at 70 eV. Optical activity was measured with a Jasco DIP-370 digital polarimeter ($\lambda =$ 589 nm). Compounds (*R*,*S*)-**12**,[8] **17**,[31] **18**,[31] and **19**[32] were obtained as reported. Silica gel plates (Merck F_{254}) and silica gel 60 (Merck 230–400 mesh) were used for analytical TLC and column chromatography, respectively. Solvents were removed under reduced pressure. All 1D and 2D NMR experiments were performed on a Varian Mercury Plus spectrometer (399.95 MHz for ^{1}H, 100.57 MHz for ^{13}C), with a 5-mm indirect detection probe equipped with a gradient coil at 298 K. Chemical shifts (δ in ppm) were referenced to the solvent CDCl₃ (7.26 ppm for ^{1}H and 77.00 ppm for ^{13}C) or [D₆]DMSO (2.50 ppm for ^{1}H and 39.50 ppm for ^{13}C). All coupling constants are in Hz. Assignments were made using ^{1}H, ^{13}C, DEPT, and NOESY 1D experiments and gHSQC, gHMBC, gHMQC, and gCOSY 2D experiments. All pulse sequences were used as provided by Varian, and processing was carried out with standard Varian software.

Synthesis of compounds 3–6, 8, and 9; typical procedure: A 2.0 M solution of lithium diisopropylamide (LDA) in *n*-heptane/THF/ethylbenzene (0.5 mL, 1.0 mmol) was added under N₂ to a solution of furanone **17** (95 mg, 0.8 mmol) in dry THF (10 mL) at −78 °C. The solution was stirred for 1 h, and the solution of ketone **19** (240 mg, 1.0 mmol) in dry THF (10 mL) was added dropwise; after 4 h the temperature was slowly increased to 10 °C. The mixture was poured onto EtOAc (25 mL) containing NH₄Cl (143 mg) and filtered. Removal of the solvent under vacuum left a yellow oil that was purified by flash chromatography (EtOAc/petroleum ether (PE, bp fraction: 40–70 °C) 3:1 as eluent, yield 65%) and identified as the corresponding aldol. Et₃N (0.5 mL, 3.6 mmol) was added to a solution of the aldol (117 mg, 0.33 mmol) in dry THF (10 mL); the mixture was refrigerated to 0 °C, and a solution of methanesulfonyl chloride (0.08 mL, 1.0 mmol) was added dropwise. The resulting suspension was stirred at 0 °C for 5 h and then filtered through a pad of silica treated with Et₂O. Removal of the solvent left a solid containing a mixture of compounds **6** and **9** that was resolved by flash chromatography (EtOAc/PE₄₀₋₇₀ 1:1 as eluent). The fastest-running band ($R_f = 0.37$) afforded 7-{[(2*Z*)-3-(5,5-dimethyl-4-oxo-4,5-dihydrofuran-2-yl)-2-methylprop-2-en-1-yl]oxy}-4-methyl-2*H*-chromen-2-one (**9**) as a white waxy solid (22%): EIMS: *m/z* (%) 340 [*M*]⁺ (10), 176 (5), 165 (25), 91 (8), 77 (55), 69 (100); ^{1}H NMR (CDCl₃): $\delta =$ 7.50 (d, ³*J* = 8.8 Hz, 1H, H-5), 6.87 (dd, ³*J* = 8.8 Hz, ⁴*J* = 2.6 Hz, 1H, H-6), 6.83 (d, ⁴*J* = 2.6 Hz, 1H, H-8), 6.22 (q, ⁴*J* = 1.3 Hz, 1H, H-3′), 6.14 (q, ⁴*J* = 1.2 Hz, 1H, H-3), 5.45 (s, 1H, H-3″), 5.095 (s, 2H, 1′-CH₂), 2.395 (d, ⁴*J* = 1.2 Hz, 3H, 4-CH₃), 2.08 (d, ⁴*J* = 1.3 Hz, 3H, 2′-CH₃), 1.43 ppm (s, 6H, 2×5″-CH₃); ^{13}C NMR (CDCl₃): $\delta =$ 206.56 (C4″), 180.81 (C2″), 161.33 (C7), 161.07 (C2), 155.24 (C8a), 152.37 (C4), 148.42 (C2′), 125.69 (C5), 117.57 (C3′), 113.99 (C4a), 112.46 (C6), 112.25 (C3), 103.54 (C3″), 101.61 (C8), 89.10 (C5″), 67.98 (C1′),
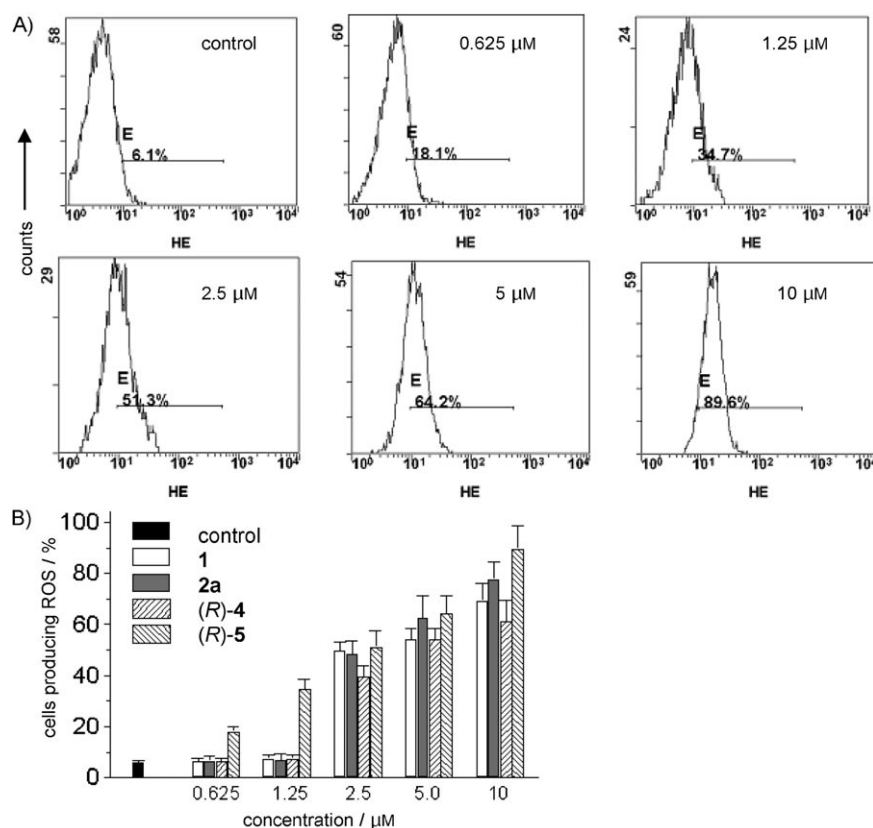
Figure 8. Mitochondrial production of ROS: A) Cells were incubated with the indicated concentrations of **1**, **2a**, (*R*)-**4**, and (*R*)-**5**, and after 24 h, cells were harvested and incubated with HE. B) Analysis of intracellular fluorescence was conducted by flow cytometry; data are represented as percentage of ethidium-positive cells and are expressed as the mean ± SEM of three independent experiments.

^{13}C NMR (CDCl$_3$): $\delta = 207.22$ (C4′′), 182.98 (C2′′), 161.18 (C2), 160.91 (C7), 155.79 (C8a), 143.39 (C4), 136.77 (C2′), 128.92 (C5), 127.17 (C3′), 113.72 (C6), 113.32 (C3), 112.81 (C4a), 102.14 (C8), 100.34 (C3′′), 88.68 (C5′′), 71.77 (C1′), 23.08 (2×5′′-CH$_3$), 20.40 (1′-CH$_3$), 13.68 ppm (3′-CH$_3$); Anal. calcd for C$_{20}$H$_{20}$O$_5$ (340.37): C 70.57, H 5.92, found: C 70.39, H 6.04. Employing DCC-CuCl in benzene at reflux for dehydration of the aldol, compound **3** was obtained in 30% yield.

7-{[(1*R*,2*E*)-3-(5,5-dimethyl-4-oxo-4,5-dihydrofuran-2-yl)-1-methyl-2-propenyl]oxy}-2*H*-chromen-2-one (*R*)-4: Overall yield: 67%, white waxy solid; $R_f = 0.35$ (EtOAc/PE$_{40-70}$ 1:1); $[\alpha]_D^{20} = +202.2$ (c = 0.46, CHCl$_3$); EIMS: *m/z* (%) 326 [*M*]$^+$ (12), 165 (62), 162 (24), 69 (100), 65 (34); ^{1}H NMR (CDCl$_3$): $\delta = 7.63$ (d, $^3J = 9.6$ Hz, 1H, H-4), 7.38 (d, $^3J = 8.5$ Hz, 1H, H-5), 6.86 (dd, $^3J = 8.5$ Hz, $^4J = 2.6$ Hz, 1H, H-6), 6.80 (d, $^4J = 2.6$ Hz, 1H, H-8), 6.78 (dd, $^3J = 15.7$ Hz, $^4J = 4.8$ Hz, 1H, H-2′), 6.43 (dd, $^3J = 15.7$ Hz, $^4J = 1.6$ Hz, 1H, H-3′), 6.26 (d, $^3J = 9.6$ Hz, 1H, H-3), 5.47 (s, 1H, H-3′′), 5.05 (qdd, $^3J = 6.4$ Hz, $^3J = 4.8$ Hz, $^4J = 1.6$ Hz, 1H, H-1′), 1.56 (d, $^3J = 6.4$ Hz, 3H, 1′-CH$_3$), 1.40 (s, 3H, 5′′-CH$_3$), 1.39 ppm (s, 3H, 5′′-CH$_3$); ^{13}C NMR (CDCl$_3$): $\delta = 206.93$ (C4′′), 179.97 (C2′′), 160.97 (C2), 160.56 (C7), 155.77 (C8a), 143.23 (C4), 140.35 (C2′), 128.93 (C5), 119.62 (C3′), 113.57 (C6), 113.49 (C3), 112.94 (C4a), 102.55 (C8), 102.44 (C3′′), 88.59 (C5′′), 73.61 (C1′), 23.03 (2×5′′-CH$_3$), 20.73 ppm (1′-CH$_3$); Anal. calcd for C$_{19}$H$_{18}$O$_5$ (326.12): C 69.93, H 5.56, found: C 70.19, H 5.87.

7-{[(1*S*,2*E*)-3-(5,5-dimethyl-4-oxo-4,5-dihydrofuran-2-yl)-1-methyl-2-propenyl]oxy}-2*H*-chromen-2-one (*S*)-4: Overall yield: 70%; white waxy solid; $[\alpha]_D^{20} = -202.0$ (c = 0.50, CHCl$_3$).

7-{[(1*R*,2*E*)-3-(5,5-dimethyl-4-oxo-4,5-dihydrofuran-2-yl)-1-methyl-2-propenyl]oxy}-4-methyl-2*H*-chromen-2-one (*R*)-5: Overall yield: 68%; white waxy solid; $R_f = 0.40$ (EtOAc/PE$_{40-70}$ 1:1); $[\alpha]_D^{20} = +272.1$ (c = 1.07, CHCl$_3$).

7-{[(1*S*,2*E*)-3-(5,5-dimethyl-4-oxo-4,5-dihydrofuran-2-yl)-1-methyl-2-propenyl]oxy}-4-methyl-2*H*-chromen-2-one (*S*)-5: Overall yield: 70%; white waxy solid; $[\alpha]_D^{20} = -272.0$ (c = 1.08, CHCl$_3$).

7-{[(2*R*,3*Z*)-4-(5,5-dimethyl-4-oxo-4,5-dihydrofuran-2-yl)pent-3-en-2-yl]oxy}-2*H*-chromen-2-one (*R*)-8: Yield: 6%, mp: 147–148 °C; $R_f = 0.5$ (EtOAc/PE$_{40-70}$ 1:1); $[\alpha]_D^{20} = -4.2$ (c = 0.30, CHCl$_3$); EIMS: *m/z* (%) 340 [*M*]$^+$ (4), 179 (47), 162 (9), 91 (14), 77 (32), 69 (100); ^{1}H NMR (CDCl$_3$): $\delta = 7.60$ (d, $^3J = 9.5$ Hz, 1H, H-4), 7.32 (d, $^3J = 8.5$ Hz, 1H, H-5), 6.76 (dd, $^3J = 8.5$ Hz, $^4J = 2.45$ Hz, 1H, H-6), 6.72 (d, $^4J = 2.45$ Hz, 1H, H-8), 6.20 (d, $^3J = 9.5$ Hz, 1H, H-3), 5.82 (dq, $^3J = 6.4$ Hz, $^4J = 1.3$ Hz, 1H, H-2′), 5.69 (pseudo-quintet, $^3J = 6.4$ Hz, 1H, H-1′), 5.57 (s, 1H, H-3′′), 1.98 (d, $^4J = 1.3$ Hz, 3H, 3′-CH$_3$), 1.48 (d, $^3J = 6.4$ Hz, 3H, 1′-CH$_3$), 1.465 (s, 3H, 5′′-CH$_3$), 1.44 ppm (s, 3H, 5′′-CH$_3$);

23.235 (2×5′′-CH$_3$), 22.32 (2′-CH$_3$), 18.64 ppm (4-CH$_3$); Anal. calcd for C$_{20}$H$_{20}$O$_5$ (340.37): C 70.57, H 5.92, found: C 70.68, H 5.90.

The second band ($R_f = 0.27$) was identified as 7-{[(2*E*)-3-(5,5-dimethyl-4-oxo-4,5-dihydrofuran-2-yl)-2-methylprop-2-en-1-yl]oxy}-4-methyl-2*H*-chromen-2-one (**6**), a white solid (40%): mp: 139–140 °C; EIMS: *m/z* (%) 340 [*M*]$^+$ (6), 176 (2), 165 (8), 91 (10), 77 (45), 69 (100); ^{1}H NMR (CDCl$_3$): $\delta = 7.53$ (d, $^3J = 8.8$ Hz, 1H, H-5), 6.91 (dd, $^3J = 8.8$ Hz, $^4J = 2.55$ Hz, 1H, H-6), 6.815 (d, $^4J = 2.55$ Hz, 1H, H-8), 6.34 (q, $^4J = 1.1$ Hz, 1H, H-3′), 6.16 (q, $^4J = 1.1$ Hz, 1H, H-3), 5.49 (s, 1H, H-3′′), 4.61 (s, 2H, 1′-CH$_2$), 2.405 (d, $^4J = 1.1$ Hz, 3H, 4-CH$_3$), 2.16 (d, $^4J = 1.1$ Hz, 3H, 2′-CH$_3$), 1.42 ppm (s, 6H, 2×5′′-CH$_3$); ^{13}C NMR (CDCl$_3$): $\delta = 207.02$ (C4′′), 181.93 (C2′′), 161.02 (C2), 160.88 (C7), 155.20 (C8a), 152.36 (C4), 146.73 (C2′), 125.78 (C5), 115.40 (C3′), 114.23 (C4a), 112.685 (C6), 112.42 (C3), 103.25 (C3′′), 101.77 (C8), 88.21 (C5′′), 72.17 (C1′), 23.16 (2×5′′-CH$_3$), 18.65 (4-CH$_3$), 16.70 ppm (2′-CH$_3$); Anal. calcd for C$_{20}$H$_{20}$O$_5$ (340.37): C 70.57, H 5.92, found: C 70.71, H 5.72.

7-{[(2*R*,3*E*)-4-(5,5-dimethyl-4-oxo-4,5-dihydrofuran-2-yl)pent-3-en-2-yl]oxy}-2*H*-chromen-2-one (*R*)-3: Overall yield: 61%, colorless crystals; $R_f = 0.34$ (EtOAc/PE$_{40-70}$ 1:1); mp: 210–211 °C; EIMS: *m/z* (%) 340 [*M*]$^+$ (3), 179 (50), 162 (5), 91 (19), 77 (22), 69 (100); ^{1}H NMR (CDCl$_3$): $\delta = 7.63$ (d, $^3J = 9.5$ Hz, 1H, H-4), 7.37 (d, $^3J = 8.6$ Hz, 1H, H-5), 6.81 (dd, $^3J = 8.6$ Hz, $^4J = 2.35$ Hz, 1H, H-6), 6.71 (d, $^4J = 2.35$ Hz, 1H, H-8), 6.54 (dq, $^3J = 7.8$ Hz, $^4J = 1.3$ Hz, 1H, H-2′), 6.25 (d, $^3J = 9.5$ Hz, 1H, H-3), 5.58 (s, 1H, H-3′′), 5.20 (dq, $^3J = 7.8$ Hz, $^3J = 6.4$ Hz, 1H, H-1′), 2.05 (d, $^3J = 1.3$ Hz, 3H, 3′-CH$_3$), 1.54 (d, $^3J = 6.4$ Hz, 3H, 1′-CH$_3$), 1.39 (s, 3H, 5′′-CH$_3$), 1.36 ppm (s, 3H, 5′′-CH$_3$);
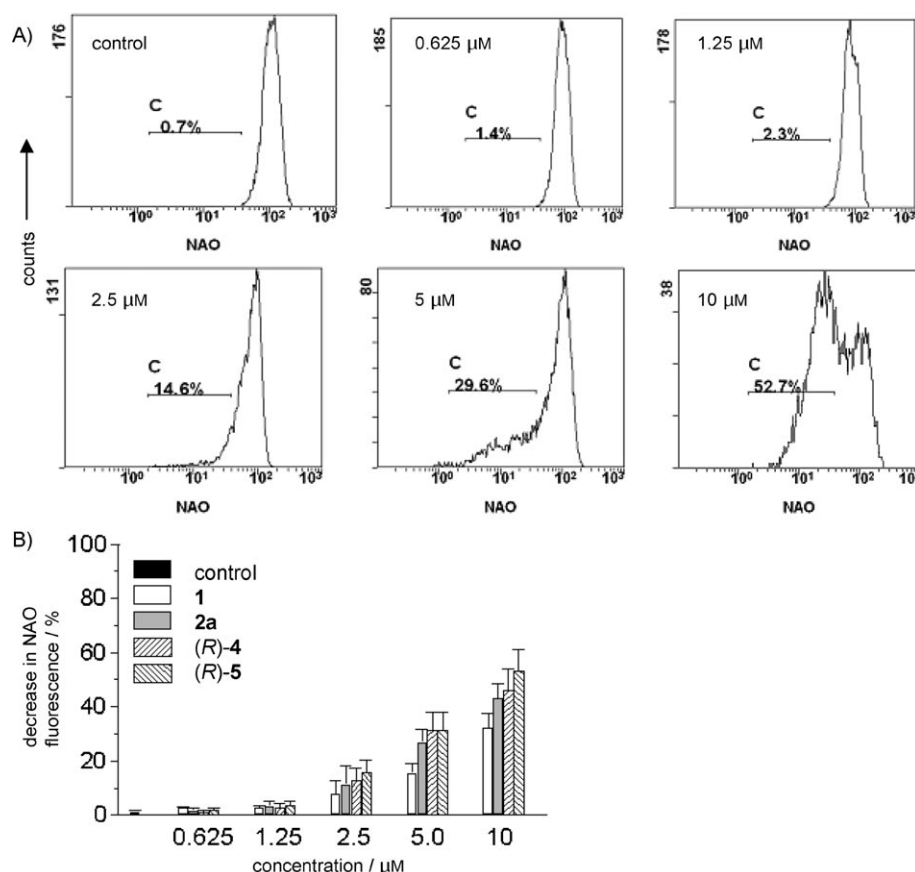
Figure 9. A) Flow cytometry histograms of NAO-loaded cells treated with compound (*R*)-**5** at the indicated concentrations and analyzed after 24 h. B) Percentage of cells with decreased NAO fluorescence after 24 h incubation with compounds **1**, **2a**, (*R*)-**4**, and (*R*)-**5** at various concentrations; data are expressed as the mean ± SEM of three independent experiments.

9.8 mmol), and (*R*)-isobutyl lactate (1.50 mL, 10.0 mmol) in anhydrous THF (20 mL) was stirred under N$_2$ at room temperature for 10 min. A solution of diisopropyl azodicarboxylate (DIAD; 1.8 mL, 9.15 mmol) in anhydrous THF (8 mL) was then added dropwise, and the resulting mixture was stirred under N$_2$ at room temperature for 2.5 h. The solvent was removed under reduced pressure, and the ester was purified by flash chromatography (EtOAc/PE$_{40–70}$ 1:2 as eluent). The obtained ester usually contained an impurity, which was removed during the workup procedure of the hydrolysis. The crude ester (3.3 g) was dissolved in CH$_3$OH (100 mL), after which 1.30 M NaOH (12.5 mL) was added, and the solution was stirred at room temperature for 2 h. After removal of the solvent, the solid was dissolved in H$_2$O (80 mL), and the aqueous phase was washed with EtOAc (5× 10 mL), cooled in an ice bath, and neutralized with 2.40 M HCl. The obtained solid was filtered and dried in vacuo in the presence of P$_2$O$_5$. The acid (*S*)-**16** (1.68 g, 6.8 mmol) was recovered in 76% overall yield. The same procedure allowed access to the acid (*R*)-**16** by replacement of (*R*)-(+)-isobutyl lactate with (*S*)-(−)-ethyl lactate.

^{13}C NMR (CDCl$_3$): δ = 206.64 (C4''), 182.99 (C2''), 161.07 (C7 and C2), 155.69 (C8a), 143.28 (C4), 140.81 (C2'), 128.72 (C5), 126.12 (C3'), 113.40 (C6), 113.02 (C3), 112.495 (C4a), 102.96 (C3''), 102.20 (C8), 88.69 (C5''), 71.99 (C1'), 23.27 (5''-CH$_3$), 22.85 (5''-CH$_3$), 21.15 (3'-CH$_3$), 20.86 ppm (1'-CH$_3$); Anal. calcd for C$_{20}$H$_{20}$O$_5$ (340.37): C 70.57, H 5.92, found: C 70.42, H 6.00. Employing DCC-CuCl in benzene at reflux for dehydration of the aldol, compound **8** could be obtained in 40% yield.

Synthesis of enantiomerically pure aldehydes 10 and 11. These compounds were prepared by following published procedures, using the enantiomerically pure acids **12** and **16** as starting materials.[9]

(2R)-[(2-oxo-2H-chromen-7-yl)oxy]propanal (R)-10: Waxy solid; $[\alpha]_D^{20}$ = +44.6 (*c* = 1.55, CH$_3$OH).

(2S)-[(2-oxo-2H-chromen-7-yl)oxy]propanal (S)-10: Waxy solid; $[\alpha]_D^{20}$ = −44.0 (*c* = 1.01, CH$_3$OH).

(2R)-[(4-Methyl-2-oxo-2H-chromen-7-yl)oxy]propanal (R)-11: Waxy solid; $[\alpha]_D^{20}$ = +57.4 (*c* = 0.87, CHCl$_3$).

(2S)-[(4-Methyl-2-oxo-2H-chromen-7-yl)oxy]propanal (S)-11: Waxy solid; $[\alpha]_D^{20}$ = −57.0 (*c* = 0.91, CHCl$_3$).

Synthesis of coumarinyloxypropionic acids 12 and 16 by Mitsunobu reaction; typical procedure: A solution of 4-methyl-7-hydroxycoumarin **15** (1.56 g, 8.9 mmol), triphenylphosphine (2.6 g,

(2R)-[(2-oxo-2H-chromen-7-yl)oxy]propanoic acid (R)-12: $[\alpha]_D^{20}$ = +91.6 (*c* = 0.84, CH$_3$OH).

(2S)-[(2-oxo-2H-chromen-7-yl)oxy]propanoic acid (S)-12: $[\alpha]_D^{20}$ = −91.1 (*c* = 0.91, CH$_3$OH).

2-[(4-Methyl-2-oxo-2H-chromen-7-yl)oxy]propanoic acid (R,S)-16: mp: 146–147 °C (lit. mp: 80–81 °C[33]); ^{1}H NMR ([D$_6$]DMSO): δ = 7.66 (d, ^3J = 8.8 Hz, 1H, H-5), 6.92 (dd, ^3J = 8.8 Hz, ^4J = 2.3 Hz, 1H, H-6'), 6.86 (d, ^4J = 2.3 Hz, 1H, H-8'), 6.20 (q, ^4J = 1.1 Hz, 1H, H-3'), 5.04 (q, ^3J = 6.8 Hz, 1H, H-2), 2.37 (d, ^4J = 1.1 Hz, 3H, 4'-CH$_3$), 1.54 ppm (d, ^3J = 6.8 Hz, 3H, 3-CH$_3$); ^{13}C NMR (CDCl$_3$): δ = 172.43 (C1), 160.46 (C7'), 160.03 (C2'), 154.49 (C8a'), 153.27 (C4'), 126.51 (C5'), 113.45 (C4a'), 112.40 (C6'), 111.37 (C3'), 101.70 (C8'), 71.89 (C2), 18.07 (4'-CH$_3$), 18.00 ppm (C3).

(2R)-[(4-Methyl-2-oxo-2H-chromen-7-yl)oxy]propanoic acid (R)-16: $[\alpha]_D^{20}$ = +78.6 (*c* = 1.05, CH$_3$OH).

(2S)-[(4-Methyl-2-oxo-2H-chromen-7-yl)oxy]propanoic acid (S)-16: $[\alpha]_D^{20}$ = −77.6 (*c* = 1.22, CH$_3$OH).

Synthesis of 13a and 13b: A mixture of acid (*R,S*)-**12** (0.400 g, 1.71 mmol) and thionyl chloride (0.87 mL, 12 mmol) was held at reflux for 2 h in dry CHCl$_3$ (15 mL). Excess thionyl chloride and CHCl$_3$ were then removed under reduced pressure to obtain the pure acyl chloride (quantitative yield). A solution of the acyl chloride (0.432 g, 1.71 mmol) in anhydrous CHCl$_3$ (6 mL) was added dropwise to a suspension of (1*R*,2*S*,5*R*)-(−)-menthol (0.267 g,

1.71 mmol), anhydrous Et$_3$N (2 mL), and a catalytic amount of 4-dimethylaminopyridine (DMAP) in anhydrous CHCl$_3$ (6 mL). The resulting mixture was heated at reflux for 4 h under N$_2$, and then cooled, diluted with CHCl$_3$ (10 mL), and washed with 3 M HCl. The organic phase was dried (Na$_2$SO$_4$), filtered, and concentrated under reduced pressure to give a yellow oil that was subjected to flash chromatography with EtOAc/PE$_{40-70}$ 1:4 as eluent. A resulting diastereomeric mixture of esters **13a** and **13b** was obtained in 84% yield (0.532 g, 1.43 mmol). Subsequent fractional crystallizations from EtOH gave pure **13b** (0.320 g, 0.86 mmol, 60%) and **13a** (0.180 g, 0.48 mmol, 34%).

(1R,2S,5R)-5-methyl-2-(propan-2-yl)cyclohexyl-(2R)-2-[(2-oxo-2H-chromen-7-yl)oxy]propanoate 13a. Colorless crystals; mp: 80–81 °C; EIMS: m/z (%) 372 [M]$^+$ (20), 234 (14), 189 (26), 175 (63), 83 (100); ^{1}H NMR (CDCl$_3$): $\delta = 7.60$ (d, $^3J = 9.5$ Hz, 1H, H-4‴), 7.37 (d, $^3J = 8.6$ Hz, 1H, H-5‴), 6.84 (dd, $^3J = 8.5$ Hz, $^4J = 2.3$ Hz, 1H, H-6‴), 6.75 (d, $^4J = 2.3$ Hz, 1H, H-8‴), 6.25 (d, $^3J = 9.5$ Hz, 1H, H-3‴), 4.80 (q, $^3J = 6.7$ Hz, 1H, H-2), 4.66 (td, $^3J = 10.8$ Hz, $^3J = 4.4$ Hz, 1H, H-1′), 2.02–1.96 (m, 1H, 6′-CHH), 1.65 (d, $^3J = 6.7$ Hz, 3H, 3-CH$_3$), 1.70–1.58 (m, 2H, 3′-CHH, 4′-CHH), 1.52–1.40 (m, 2H, H-5′, H-2″), 1.40–1.30 (m, 1H, H-2′), 1.09–0.91 (m, 2H, 6′-CHH, 3′-CHH), 0.90 (d, $^3J = 6.4$ Hz, 3H, 5′-CH$_3$), 0.90–0.78 (m, 1H, 4′-CHH), 0.71 (d, $^3J = 6.7$ Hz, 3H, 1″-CH$_3$), 0.57 ppm (d, $^3J = 7.0$ Hz, 3H, 3″-CH$_3$); ^{13}C NMR (CDCl$_3$): $\delta = 170.98$ (C1), 161.01 (C2‴), 160.85 (C7‴), 155.74 (C8a‴), 143.20 (C4‴), 128.91 (C5‴), 113.63 (C4a‴), 113.10 (C6‴), 112.94 (C3‴), 102.10 (C8‴), 75.95 (C1′), 73.09 (C2), 46.78 (C2′), 40.58 (C6′), 34.09 (C4′), 31.42 (C5′), 25.78 (C2″), 22.95 (C3′), 21.96 (5′-CH$_3$), 20.71 (C1″), 18.44 (C3), 15.71 ppm (C3″); Anal. calcd for C$_{22}$H$_{28}$O$_5$ (372.45): C 70.94, H 7.58, found: C 71.05, H 7.44.

(1R,2S,5R)-5-methyl-2-(propan-2-yl)cyclohexyl-(2S)-2-[(2-oxo-2H-chromen-7-yl)oxy]propanoate 13b: Colorless crystals; mp: 129–130 °C; EIMS: m/z (%) 372 [M]$^+$ (13), 234 (26), 189 (40), 175 (35), 83 (100); ^{1}H NMR (CDCl$_3$): $\delta = 7.62$ (d, $^3J = 9.5$ Hz, 1H, H-4‴), 7.36 (d, $^3J = 8.6$ Hz, 1H, H-5‴), 6.83 (dd, $^3J = 8.6$ Hz, $^4J = 2.5$ Hz, 1H, H-6‴), 6.75 (d, $^4J = 2.5$ Hz, 1H, H-8‴), 6.26 (d, $^3J = 9.5$ Hz, 1H, H-3‴), 4.78 (q, $^3J = 6.8$ Hz, 1H, H-2), 4.77 (td, $^3J = 11.0$ Hz, $^3J = 4.4$ Hz, 1H, H-1′), 1.95–1.84 (m, 2H, H-2″, 6′-CHH), 1.71–1.60 (m, 2H, 4′-CHH, 3′-CHH), 1.64 (d, $^3J = 6.8$ Hz, 3H, 2-CH$_3$), 1.50–1.36 (m, 2H, H-5′, H-2′), 1.10 (m, 1H, 3′-CHH), 0.96–0.80 (m, 2H, 4′-CHH, 6′-CHH), 0.93 (d, $^3J = 7.0$ Hz, 3H, 1″-CH$_3$), 0.86 (d, $^3J = 6.5$ Hz, 3H, 5′-CH$_3$), 0.76 ppm (d, $^3J = 7.0$ Hz, 3H, 3″-CH$_3$); ^{13}C NMR (CDCl$_3$): $\delta = 170.70$ (C1), 160.85 (C2‴), 160.61 (C7‴), 155.55 (C8a‴), 143.10 (C4‴), 128.76 (C5‴), 113.56 (C4a‴), 113.06 (C6‴), 112.84 (C3‴), 102.20 (C8‴), 75.70 (C1′), 72.92 (C2), 46.86 (C2′), 40.46 (C6′), 34.09 (C4′), 31.34 (C5′), 26.43 (C2″), 23.27 (C3′), 21.96 (5′-CH$_3$), 20.76 (C1″), 18.34 (C3), 16.07 ppm (C3″); Anal. calcd for C$_{22}$H$_{28}$O$_5$ (372.45): C 70.94, H 7.58, found: C 71.03, H 7.68.

X-ray crystal structure analysis for 13b: Formula: C$_{44}$H$_{54}$O$_{10}$, $M_r =$ 742.87 Da, colorless crystal, monoclinic, space group: P21/a, $a =$ 10.631(5), $b = 11.431(5)$, $c = 17.699(5)$ Å, $\alpha = 90.000(5)°$, $\beta =$ 106.040(5)°, $\gamma = 90.000(5)°$, $V = 2067(15)$ Å^3, $Z = 2$, $T = 293(2)$ K, $\mu =$ 0.68 mm^{-1}, $F(000) = 796$; 4050 reflections were collected in the range $2.60° < \theta < 60.03°$; the final R index was 0.0421 for reflections with $I > 2\sigma(I)$. CCDC 701551 contains the supplementary crystallographic data for this paper. These data can be obtained free of charge from The Cambridge Crystallographic Data Centre via http://www.ccdc.cam.ac.uk/data_request/cif.

Hydrolysis of esters 13a and 13b. An aqueous solution of NaOH (10%, 0.5 mL) was added under N$_2$ to a solution of the ester **13a** or **13b** (0.164 g, 0.44 mmol) in CH$_3$CN (6 mL), and the resulting mixture was stirred at room temperature for 5 days. The solvent was removed under reduced pressure, and the residue was suspended in H$_2$O. The resulting suspension was acidified with 10% HCl and extracted with CH$_2$Cl$_2$. The organic phase was dried and concentrated under reduced pressure to give a solid that was subject to flash chromatography with EtOAc/PE$_{40-70}$ 1:4 as eluent. The recovered acid wad dissolved in H$_2$O (25 mL) and 2.4 M HCl was added, under cooling, until the pH became acidic. The acid (R)-**12** or (S)-**12** was filtered and dried (76 mg, 0.32 mmol, 74%; (R)-**12** $[\alpha]_D^{20} = +90.3$ ($c = 0.82$, CH$_3$OH); (S)-**12** $[\alpha]_D^{20} = -89.8$ ($c = 0.80$, CH$_3$OH)).

Synthesis of 14a and 14b. A mixture of acid (R,S)-**12** (0.112 g, 0.48 mmol) and thionyl chloride (0.25 mL, 3.44 mmol) was held at reflux for 2 h in dry CHCl$_3$ (10 mL). Excess thionyl chloride and CHCl$_3$ were then removed under reduced pressure to obtain the pure acyl chloride in quantitative yield. (R)-(+)-α-methylbenzylamine (0.25 mL, 2 mmol) was added to a solution of acyl chloride in anhydrous CHCl$_3$ (10 mL). The resulting solution was heated at reflux for 1 h under N$_2$; after cooling to room temperature, the solution was stirred overnight under N$_2$. The solvent was removed under reduced pressure, and the residue was purified by flash chromatography in EtOAc/PE$_{40-70}$ 1:1 as eluent (0.136 g, 0.40 mmol, 84%). **14a** and **14b** were obtained by subsequent fractional crystallizations from CH$_3$OH/H$_2$O (2:1).

(2R)-2-[(2-oxo-2H-chromen-7-yl)oxy]-N-[(1R)-1-phenylethyl]-propanamide 14a. Yield, 40%; mp: 114–115 °C; EIMS: m/z (%) 337 [M]$^+$ (14), 189 (40), 176 (35), 105 (100); ^{1}H NMR (CDCl$_3$): $\delta = 7.62$ (d, $^3J = 9.5$ Hz, 1H, H-4‴), 7.34 (d, $^3J = 9.3$ Hz, 1H, H-5‴), 7.21–7.17 (m, 3H, H-2″, H-4″), 7.12–7.09 (m, 2H, H-3″), 6.80–6.77 (m, 2H, H-6, H-8‴), 6.48 (d, $^3J = 8.6$ Hz, 1H, NH), 6.29 (d, $^3J = 9.5$ Hz, 1H, H-3‴), 5.13 (pseudo-quintet, $^3J = 7.8$ Hz, 1H, H-1′), 4.73 (q, $^3J = 6.7$ Hz, 1H, H-2), 1.64 (d, $^3J = 6.7$ Hz, 3H, 2-CH$_3$), 1.51 ppm (d, $^3J = 7.8$ Hz, 3H, 1′-CH$_3$); ^{13}C NMR (CDCl$_3$): $\delta = 170.37$ (C1), 160.07 (C2‴), 159.78 (C7‴), 155.56 (C8a‴), 142.96 (C4‴), 142.48 (C1″), 129.09 (C5‴), 128.54 (C3″), 127.35 (C4″), 125.89 (C2″), 114.10 (C3‴), 113.58 (C4a‴), 112.40 (C6‴), 103.42 (C8‴), 75.47 (C2), 48.39 (C1′), 21.57 (1′-CH$_3$), 18.55 ppm (2-CH$_3$); Anal. calcd for C$_{20}$H$_{19}$NO$_4$ (337.37): C 71.20, H 5.68, N 4.15, found: C 71.01, H 5.79, N 4.35.

(2S)-2-[(2-oxo-2H-chromen-7-yl)oxy]-N-[(1R)-1-phenylethyl]-propanamide 14b. Yield, 25%; mp: 135–136 °C; EIMS: m/z (%) 337 [M]$^+$ (12), 189 (26), 176 (46), 105 (100); ^{1}H NMR (CDCl$_3$): $\delta = 7.64$ (d, $^3J = 9.6$ Hz, 1H, H-4‴), 7.41 (d, $^3J = 9.4$ Hz, 1H, H-5‴), 7.38–7.32 (m, 2H, H-3″), 7.31–7.25 (m, 3H, H-2″, H-4″), 6.88–6.83 (m, 2H, H-6, H-8‴), 6.51 (d, $^3J = 8.2$ Hz, 1H, NH), 6.30 (d, $^3J = 9.6$ Hz, 1H, H-3‴), 5.15 (pseudo-quintet, $^3J = 7.0$ Hz, 1H, H-1′), 4.76 (q, $^3J = 6.9$ Hz, 1H, H-2), 1.58 (d, $^3J = 6.9$ Hz, 3H, 2-CH$_3$), 1.41 ppm (d, $^3J = 7.0$ Hz, 3H, 1′-CH$_3$); ^{13}C NMR (CDCl$_3$): $\delta = 170.02$ (C1), 160.70 (C2‴), 159.77 (C7‴), 155.69 (C8a‴), 142.99 (C4‴), 142.52 (C1″), 129.15 (C5‴), 128.79 (C3″-C5″), 127.56 (C4″), 126.01 (C2″-C6″), 114.17 (C3‴), 113.67 (C4a‴), 112.47 (C6‴), 103.36 (C8‴), 75.59 (C2), 48.38 (C1′), 21.58 (1′-CH$_3$), 18.51 ppm (2-CH$_3$); Anal. calcd for C$_{20}$H$_{19}$NO$_4$ (337.37): C 71.20, H 5.68, N 4.15, found: C 71.08, H 5.70, N 4.24.

Hydrolysis of amides 14a and 14b. A suspension of the amide **14b** (155 mg, 0.46 mmol) in a solution of 6 M HCl (6 mL) was heated at reflux for 15 h. After cooling to room temperature, the solution was extracted with CH$_2$Cl$_2$ (3×5 mL), and the combined organic extracts were dried over anhydrous MgSO$_4$. The organic solvent was evaporated under reduced pressure to give (S)-**12** as a yellow solid (100 mg, 0.43 mmol, 93%, $[\alpha]_D^{20} = -88.8$ ($c = 0.8$, CH$_3$OH).

Cell cultures. Leukemic human T-lymphocytes (Jurkat and CEM), human promyelocytic leukemia cells (HL-60), and human chronic

↖↖ These are not the final page numbers!

myelogenous leukemia cells (K562) were grown in RPMI-1640 medium, (Sigma–Aldrich, Milan, Italy). Human intestinal adenocarcinoma (LoVo) cells were grown in Ham's F-12 medium (Sigma–Aldrich), and human fibrosarcoma (HT-1080) and breast adenocarcinoma (MCF7) cells were grown in Dulbecco's modified Eagle's medium (DMEM; Sigma–Aldrich), all of which were supplemented with penicillin G (115 U mL^{-1}; Invitrogen, Milan, Italy), streptomycin (115 µg mL^{-1}; Invitrogen), and fetal bovine serum (10%; Invitrogen). LoVo/Doxo cells are a doxorubicin-resistant subclone of the LoVo cell line,[13,14] and were grown in complete Ham's F-12 medium supplemented with doxorubicin (0.1 µg mL^{-1}). CEM-VBL10 is a multidrug-resistant cell line selected against vinblastine.[15] MCF7-MDR is a human mammary carcinoma cell line that exhibits multidrug resistance and high levels of P-gp expression.[16,17] They were grown in complete DMEM supplemented with doxorubicin (0.1 µg mL^{-1}).

Cell-cycle analysis. For flow cytometric analysis of DNA content, 5×10^5 HL-60 cells in exponential-phase growth were treated with the test compounds for 24 h. After this incubation period, cells were centrifuged and fixed with ice-cold EtOH (70%), treated with lysis buffer containing RNAse A, and then stained with propidium iodide (PI). Samples were analyzed on a Beckman-Coulter Epics XL-MCL flow cytometer. For cell-cycle analysis, DNA histograms were analyzed using MultiCycle for Windows (Phoenix Flow Systems, USA)

Externalization of phosphatidylserine. Surface exposure of phosphatidylserine (PS) by apoptotic cells was measured by flow cytometry with a Beckman-Coulter Cytomics FC500 (Beckman-Coulter, USA) by adding annexin V–FITC to cells according to the manufacturer's instructions (Annexin V Fluos, Roche Diagnostics). The cells were simultaneously stained with PI. Excitation was set at 488 nm, and the emission filters were set at 525 and 585 nm.

Assessment of mitochondrial changes. The change in mitochondrial transmembrane potential ($\Delta\psi_{mt}$) was measured with the lipophilic cation 5,5′,6,6′-tetrachloro-1,1′,3,3′-tetraethylbenzimidazolcarbocyanine (JC-1, Molecular Probes, USA) as described.[34] Briefly, after 24 h treatment, cells were collected by centrifugation and resuspended in Hank's balanced salt solution (HBSS) containing the JC-1 at 1 µM. The cells were then incubated for 10 min at 37 °C, centrifuged, and resuspended in HBSS. The production of ROS and the oxidation of cardiolipin were measured by flow cytometry using hydroethidine (HE, Molecular Probes, USA) and 10-*N*-nonyl-acridine orange (NAO, Molecular Probes, USA), respectively. After 24 h treatment, the cells were collected by centrifugation and resuspended in HBSS containing HE (2.5 µM) or NAO (100 nM). The cells were then incubated for 30 min at 37 °C, centrifuged, and resuspended in HBSS. The fluorescence was recorded directly with the flow cytometer using an excitation wavelength of 488 nm and emission wavelengths of 585 and 530 nm for HE and NAO, respectively.

Acknowledgements

[1] K. Padmawinata, *Acta Pharm.* **1973**, *4*, 1–9.

[2] P. J. Jeri, A. B. Smith III, *J. Org. Chem.* **1981**, *46*, 577–585.

[3] P. Valenti, *Fitoterapia* **1997**, *68*, 115–126.

[4] D. Simoni, S. Manfredini, M. A. Tabrizi, R. Bazzanini, P. G. Baraldi, J. Balzarini, E. De Clercq, *J. Med. Chem.* **1991**, *34*, 3172–3176.

[5] P. G. Baraldi, S. Manfredini, D. Simoni, M. A. Tabrizi, J. Balzarini, E. De Clercq, *J. Med. Chem.* **1992**, *35*, 1877–1882.

[6] S. Manfredini, P. G. Baraldi, R. Bazzanini, M. Guarneri, D. Simoni, J. Balzarini, E. De Clercq, *J. Med. Chem.* **1994**, *37*, 2401–2405.

[7] S. Chimichi, M. Boccalini, B. Cosimelli, G. Viola, D. Vedaldi, F. Dall'Acqua, *Tetrahedron Lett.* **2002**, *43*, 7473–7476.

[8] G. Viola, D. Vedaldi, F. Dall'Acqua, G. Basso, S. Disarò, M. Spinelli, B. Cosimelli, M. Boccalini, S. Chimichi, *Chem. Biodiversity* **2004**, *1*, 1265–1280.

[9] S. Chimichi, M. Boccalini, B. Cosimelli, *Tetrahedron* **2002**, *58*, 4851–4858.

[10] S. Chimichi, M. Boccalini, G. Cravotto, O. Rosati, *Tetrahedron Lett.* **2006**, *47*, 2405–2408.

[11] O. Mitsunobu, *Synthesis* **1981**, 1–28.

[12] a) M. Solinas, S. Gladiali, M. Marchetti, *J. Mol. Catal. A* **2005**, *226*, 141–147; b) C. Basoli, C. Botteghi, M. A. Cabras, G. Chelucci, M. Marchetti, *J. Organomet. Chem.* **1995**, *488*, C20-C22.

[13] M. Grandi, C. Geroni, F. C. Giuliani, *Br. J. Cancer* **1986**, *54*, 515–518.

[14] G. Toffoli, A. Viel, L. Tumiotto, G. Biscontin, C. Rossi, M. Baiocchi, *Br. J. Cancer* **1991**, *63*, 51–56.

[15] M. L. Dupuis, M. Flego, A. Molinari, M. Cianfriglia, *HIV Med.* **2003**, *4*, 338–345.

[16] J. M. Gudas, H. Nguyen, T. Li, L. Sadzewicz, R. Robey, K. Wosikowksi, K. H. Cowan, *Carcinogenesis* **1996**, *17*, 1417–1427.

[17] G. Batist, A. Tulpule, B. Sinha, A. Katki, C. Myers, K. Cowan, *J. Biol. Chem.* **1986**, *261*, 15544–15549.

[18] S. J. Martin, C. P. Reutelingsperger, A. J. McGahon, J. A. Rader, R. C. van Schie, D. M. Laface, D. R. Green, *J. Exp. Med.* **1995**, *182*, 1545–1556.

[19] I. Vermes, C. Haanen, H. Steffens-Nakken, C. Reutelingsperger, *J. Immunol. Methods* **1995**, *184*, 39–51.

[20] C. Bocca, L. Gabriel, A. Miglietta, *Chem.-Biol. Interact.* **2001**, *137*, 285–305.

[21] J. D. Ly, D. R. Grubb, A. Lawen, *Apoptosis* **2003**, *8*, 115–128.

[22] D. R. Green, G. Kroemer, *Science* **2004**, *305*, 626–629.

[23] S. Salvioli, A. Ardizzoni, C. Franceschi, A. Cossarizza, *FEBS Lett.* **1997**, *411*, 77–82.

[24] N. Zamzami, P. Marchetti, M. Castedo, A. Decaudin, A. Macho, T. Hirsch, S. A. Susin, P. X. Petit, B. Mignotte, G. Kroemer, *J. Exp. Med.* **1995**, *182*, 367–377.

[25] J. Cai, D. P. Jones, *J. Biol. Chem.* **1998**, *273*, 11401–11404.

[26] H. Nohl, L. Gille, K. Staniek, *Biochem. Pharmacol.* **2005**, *69*, 719–723.

[27] G. Rothe, G. Valet, *J. Leukocyte Biol.* **1990**, *47*, 440–448.

[28] L. Benov, L. Sztejnberg, I. Fridovich, *Free Radical Biol. Med.* **1998**, *25*, 826–831.

[29] J. M. Petit, A. Maftah, M. H. Ratinaud, R. Julien, *Eur. J. Biochem.* **1992**, *209*, 267–273.

[30] P. F. Gallet, A. Maftah, J. M. Petit, M. Denis-Gay, R. Julien, *Eur. J. Biochem.* **1995**, *228*, 113–119.

[31] S. Chimichi, M. Boccalini, B. Cosimelli, F. Dall'Acqua, G. Viola, *Tetrahedron* **2003**, *59*, 5215–5223.

[32] R. Sicard, L. S. Chen, A. J. Marsaioli, J.-L. Reymond, *Adv. Synth. Catal.* **2005**, *347*, 1041–1050.

[33] E. Massarani, D. Nardi, F. Barzaghi, F. Bonacina, *Farmaco Ed. Sci.* **1963**, *18*, 254–267.

[34] G. Viola, E. Fortunato, F. Cecconet, F. Dall'Acqua, G. Basso, *Toxicol. Appl. Pharmacol.* **2008**, *227*, 84–96.

FULL PAPERS

S. Chimichi, M. Boccalini, A. Salvador,
F. Dall'Acqua, G. Basso, G. Viola*

■■ – ■■

Synthesis and Biological Evaluation of New Geiparvarin Derivatives
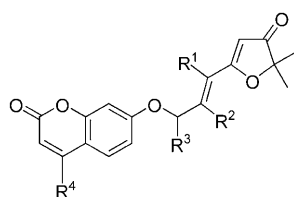
1: R^1=Me, R^2=H, R^3=H, R^4=H
(geiparvarin)
2a: R^1=H, R^2=H, R^3=H, R^4=H
(*R*)-**4**: R^1=H, R^2=H, R^3=Me, R^4=H
(*R*)-**5**: R^1=H, R^2=H, R^3=Me, R^4=Me

New geiparvarin derivatives modified at the alkenyloxy bridge, where the 3'-methyl group was replaced by a hydrogen atom, were synthesized and evaluated against a panel of human tumor cell lines in vitro. Compounds (*R*)-**4** and (*R*)-**5** show greater inhibitory activity toward cell growth than the parent geiparvarin.

↖↖ These are not the final page numbers!